Numerical Modelling of Carbon Dioxide Plume Dispersion in Sandstone Aquifer of Malay Basin

Izzat Zulfadhli Abd Rahman[1], *Dayang Zulaika* Abang Hasbollah[*2], *Brenda* Leong[1], *Aniza* Ibrahim[3], *Bakhtiar Affandy* Othman[2], *Aizat* Mohd Taib[4], *Mohd Firdaus* Md Dan @ Azlan[5], and *Hooi Chie* Lee[6]

[1]Department of Geotechnics and Transportation, Faculty of Civil Engineering, Universiti Teknologi Malaysia, 81310 Johor Bahru, Malaysia
[2]Centre of Tropical Geoengineering, Universiti Teknologi Malaysia, 81310 Johor Bahru, Malaysia
[3]Department of Civil Engineering, Faculty of Engineering, Universiti Pertahanan Nasional Malaysia, Kem Sg. Besi, 57000, Kuala Lumpur Malaysia
[4]Department of Civil Engineering, Faculty of Civil Engineering and Built Environment, Universiti Kebangsaan Malaysia, 43600 UKM Bangi, Selangor, Malaysia
[5]Sustainable Geostructure and Underground Exploration, Faculty of Civil Engineering and Built Environment, Universiti Tun Hussein Onn Malaysia, 86400 Batu Pahat, Johor, Malaysia
[6]Global Water Consultants Sdn Bhd, Kuala Lumpur, Malaysia

Abstract. 256.05 million tonnes of carbon dioxide (CO_2) have been released into the atmosphere of Malaysia as of 2021. If no steps are done to limit Malaysia's CO_2 emissions, it is projected that this scenario could go on for relatively many years to come. The feasibility of CO_2 geological sequestration has been taken into consideration as a viable method of minimizing CO_2 emission in Malaysia, considering the anticipated rise in energy demand for sustainable development in this nation. The long-term fate of the captured CO_2 is, however, the primary concern of public and environment but it is not practical to do simulations in a lab or via experiments. In examining the movement of the CO_2 plume after being injected into the sandstone aquifer, computer simulation is therefore more practical to utilize in this research. Malay Basin was ranked as the most potential basin for carbon sequestration in Malaysia because it fulfils most of the criteria. Therefore, by utilizing data from previous studies, 10 km^2 of Malay Basin sandstone aquifer was simulated using COMSOL Multiphysics software in order to explore the pattern of CO_2 dispersion in sandstone aquifer and to predict its migration radius in a given period. The second goal of this research is to determine a relationship between the rate of CO_2 injection per 10 km^2 and the velocity of CO_2 plume flow in sandstone aquifer. Lastly, this study aims to estimate the saturation of CO_2 per 10 km^2 of the aquifer with various injection rates after a given time. Results from the numerical computation shows that CO_2 injected into the Malay Basin migrates upward and laterally, with the plume pattern expanding over time and higher injection rates. On the other hand, the velocity of plume dispersion fluctuates and decreases with distance due to pressure gradients and dissolution of CO_2 into the formation's brine. Saturation of CO_2 was

Corresponding author: dzulaika@utm.my

also found to be the highest at the injection point and broadens with higher injection rates. This study's findings have practical implications for optimizing design, managing injection rates, assessing caprock integrity, implementing monitoring strategies, and conducting environmental impact assessments to ensure safe and effective carbon storage for long-term CO_2 sequestration in Malay Basin. Given the size of Malaysia's geological CO_2 sequestration industry, this research is seen as a wise investment from an economic standpoint. Politically speaking, the findings of this research provide policymakers and legislators with a suitable point of reference for implementing CO_2 emission regulations in Malaysia.

Keywords: *Carbon Dioxide Sequestration, Geological Carbon Sequestration, Malay Basin, COMSOL Multiphysics, Deep Saline Aquifer*

1 Introduction

Humanity is in danger from the disastrous effects of global warming. The common snow and ice melting, an increase in world average ocean and air surface temperatures and rising sea levels are significant impacts of global warming [4]. The world's continuous dependence on fossil fuels and the relatively slow rate of development of renewable energy sources predict that greenhouse gas emissions into the atmosphere will continue to rise. Therefore, it is essential that solutions be developed to eliminate these pollutant gases from the environment. Carbon capture and sequestration (CCS) technology's introduction, advancement, and adoption promise to minimize the quantity of greenhouse gases that enter the environment [6]. Carbon capture and sequestration (CCS) is a general term for any technique that redirects carbon to a viable carbon sink and eliminates or reverses the emission of CO2 into the atmosphere [7]. There have been several CO2 storage techniques utilized around the world. The most popular sequestration technology is geological sequestration. It is the process of injecting carbon dioxide into relatively deep (greater than 1 km) geologic formations with the sole objective of suppressing carbon dioxide emitted into the atmosphere [8]. Saline aquifers, depleted oil and gas reservoirs, and unmineable coal beds are some of these subsurface geological formations [9]. This comprehensive study will focus primarily of CO2 storage in geological formations, with a particular emphasis on sandstone aquifers that are saline.

Geological carbon sequestration involves three crucial phases which are CO2 capture, transport, and storage. The first step focuses on capturing CO2 emissions from industrial processes or power plants before they are released into the atmosphere. Different capture technologies are used depending on the emission source. Pre-combustion capture is one of the methods; fossil fuels are converted into a mixture of hydrogen and CO2 before combustion. The CO2 is then separated from the hydrogen and captured. Next capturing method is post-combustion capture, here, CO2 is captured from the flue gases emitted after combustion. Various techniques, such as chemical solvents or adsorbents, are used to selectively capture CO2 from the flue gas stream. Lastly is the oxy-fuel combustion, in this approach, fossil fuels are burned in pure oxygen, resulting in a flue gas consisting mainly of CO2 and water vapor. The CO2 can be separated and captured from this concentrated stream. The captured CO2 is then subjected to purification processes to remove impurities, ensuring its quality for subsequent storage. Once the CO2 is captured and purified, it needs to be transported to suitable storage sites. This involves the construction of pipelines or other transportation infrastructure. The CO2 is compressed into a supercritical state, where it has the properties of both a gas and a liquid, to facilitate efficient and cost-effective transport over long distances. Pipeline networks are built to connect the capture sources with the storage sites, similar to existing natural gas or oil pipeline systems. In cases where pipelines are not feasible, alternative transportation methods such as ships or trucks may be employed for shorter distances or to reach locations without pipeline access. The final step is the injection and storage of CO2 into geological formations deep underground. Various types of geological formations can be utilized for storage but our study will focus on storage in deep saline aquifers.

Saline aquifers are massive, deep formations of porous rocks. These are essentially porous sandstones and limestones that have a lot of brine water inside of them. They are surrounded on top by a caprock, a rock layer with low permeability. A rock with low permeability may also constrain them below [10]. During the carbon sequestration process, the CO2 is first compressed to an extremely high pressure, after which it is injected into saline aquifers, replacing the aquifer water with the CO2 that fills the porous area [11]. Saline aquifers have been regarded as having the greatest potential for CO2 storage due to their large capacity of 1000–10,000 Gt of CO2, which is 99% of the total global storage capacity [12]. It represents the best sequestering modes for storage of CO2 among all geological options due to their enormous storage capacity [13].

Sequestration processes are commonly divided into four different categories: hydrodynamic trapping, residual trapping, solubility trapping, and mineral trapping. For hydrodynamic trapping, CO2 is trapped as a supercritical fluid or gas under a low permeability caprock. Due to its lower density than the formation fluid, carbon dioxide will ascend buoyantly until it encounters a caprock that possesses a capillary entry pressure that is larger than the buoyancy and perhaps hydrodynamic force. This mechanism is crucial since it is a need for every storage site because it stops CO2 from leaking through the caprock while waiting for other trapping modes to take action [14]. Next, the process by which CO2 and water travel along the reservoir via buoyancy effect and water fills the pores that were previously filled by CO2 leaving bubbles of CO2 trapped in the rock pores is called residual or capillary trapping [15]. Other than that, the mechanism through which CO2 is dissolved into the brine or salt water in the rock formation is termed as solubility trapping. Whether it is in the supercritical or gaseous phase, CO2 may dissolve in other liquids. The dissolving of the CO2 in the saline water causes solubility trapping, which results in dense CO2-saturated brine. Lastly is the mineral trapping in which CO2 dissolved in native water and interacts with minerals as well as other dissolved components to generate new carbonate minerals.

With a ranking score of 0.81, [16] identified the Malay Basin as the sedimentary basin in Malaysia with the highest potential for geological storage of CO2. The Malay Basin is part of the Mesozoic continental centre of Southeast Asia and lies beneath the region known as Sundaland. It is situated in the southern section of the Gulf of Thailand across Peninsular Malaysia and Vietnam. The basin is thought to be asymmetric across its extent and cross section, measuring roughly 500 km in length with breadth of 200 km. Groups D and E of the Malay Basin strata are believed to be the best sediments for CO2 sequestration. This is because these groups are situated between 1000 and 1500 m below the surface, which is advantageous given that the Malay Basin is a warm geological basin. Therefore, injection at this depth can offer secure long-term CO2 storage since CO2 at this depth will be in its dense phase, which will increase storage volume. Additionally, Groups D and E are composed of sandstones that make up a significant group of aquifers in the Malay Basin's central region. With an estimated 17% porosity and a permeability of 40mD, Groups D and E meet the depth criteria for a safe storage unit and have good qualities for a CO2 storage aquifer [17]. Carbon sequestration plays a pivotal role in mitigating global CO2 emissions. The Malay Basin was selected due to its high ranking for carbon storage potential (score of 0.81) and favorable geological characteristics, such as the presence of sandstone aquifers with ideal porosity (17%) and permeability (40 mD). This linkage emphasizes how regional studies contribute to global CCS strategies.

Warm basins possess a surface temperature of about 20°C and geothermal gradients of about 45°C/km. The recommended depth for CO2 storage is more than 800 metres below surface. It is possible to categorise the depth at which injection takes place as "shallow" for values up to 1000 m or "deep" for depths of about 3000 m. For the sake of this analysis, the injection depth is considered to be 1000 m, corresponding to "warm" basin temperatures of 65°C. This depth was chosen because it is within the ideal depth range for CO2 sequestration (800–3000 m), where the gas injected can remain in a supercritical state, allowing for greater gas injection into a given size of the aquifer [18]. In saline aquifers, [19] reported pressure gradient of approximately 18.1 kPa/m, which, given that the pressure at the surface is 101.325 kPa or 1 atm, this corresponds to 18.1 MPa of pressure at depth of 1000 m. Depending on the structures and compositions of the sedimentary strata, this pressure gradient may change.

At pressures and temperatures greater than 31.1 °C and 7.38 MPa, CO2 often exists in the supercritical state where it behaves like a gas by occupying the entire volume yet possessing a liquid density that varies with pressure and temperature. CO2 has a density of 1.872 kg/m3 and is a stable gas in normal atmospheric settings. Supercritical CO2 can be kept in large amounts and can rapidly fill every available space because it possesses a high density more like liquid that ranges between 150 kg/m3 to over 800 kg/m3, yet it travels like a gas [20]. The temperature and pressure regime influences the density of subsurface CO2 storage. CO2 density gradually rises with depth and then stabilizes when normal settings are accounted. Carbon dioxide must be kept in a supercritical state to be successfully stored. In principle, the increased density of CO2 necessitates storage at this condition, which lowers the buoyancy difference between CO2 and the formation fluids.

The large percentage of modelling and monitoring, studies are conducted during the planning, construction, and monitoring phases of carbon dioxide storage in order to avoid leakage of gas into the atmosphere, groundwater aquifers, shallow soil regions, and beneath resource-bearing strata as well as to ensure the gas is stored safely [9]. The potential for CO2 sequestration in the geological strata of the German state of North Rhine Westphalia is examined by [21]. The numerical simulator TOUGHREACT is used to run simulations for assessing a probable site within the Bunter sandstone formation close to the city of Minden at a depth of around 3,000 m. Three CO2 storage mechanisms—hydrodynamic trapping, dissolution trapping, and mineral trapping—are the focus of their research. Using the COMET 3 numerical simulator, [22] effectively simulated the CO2 storage process in deep saline aquifers. In general, two things have been taken into account: the ability of the saline aquifer to store CO2 and the variables affecting it, as well as the potential for injected CO2 escape into the environment and the factors impacting it. Numerical modelling permits time saving and less utilization of resources for quantitative analysis of thermodynamic and geo-mechanical formation for various CCS practices. Numerous numerical models have been developed and put forward for analysis of geochemical evaluation of the CO2 injection. [23] conducted a detailed analysis of these numerical simulators and concluded that while the existing simulators generally concurred, there were significant inconsistencies due to the various fluid property models. A significant limitation of this study is the exclusion of CO2-brine dissolution effects. This omission may result in an overestimation of CO2 plume migration distances and underestimation of long-term trapping efficiency. Future studies should incorporate dissolution mechanisms to provide more comprehensive insights.

2 Methodology

This research consisted of three key activities: development of Malay Basin and injection well model in COMSOL, setting up the Multiphysics component, and parametric studies.

2.1 Model Definition.

The part of the reservoir included in the simulation to represent the sandstone aquifer of Malay Basin measures 10,000 m by 10,000 m, with a thickness of 500 m. The porosity and permeability data are obtained from the study conducted by [24]. The injection well is located at x = 5,000 m and y = 5,000 m which is placed at the center of the geometry built. CO2 is injected at a depth of 1000 km below the ground. The simulation runs over a period of 100 years. In the first 50 years, CO2 is injected at a constant rate and in the subsequent 50 years, the simulation tracks the spreading of the CO2 due to gravity and capillary forces. This simulation is repeated using different CO2 injection rates which are 25 kg/s, 50 kg/s, 75 kg/s and 100 kg/s.

The initial conditions for the simulation are a brine filled reservoir at a hydrostatic pressure distribution (hydraulic head of 0 m). The pressure boundary conditions are a hydraulic head of 0 m at the sides, and no flow at the top and bottom boundaries. CO2 saturation is 0 at the side boundaries. The time constant geothermal gradient is taken to be 45°C/km with a temperature of 65°C at a depth of 1000 m. The pressure and temperature dependent density and viscosity of the supercritical CO2 are computed using the thermodynamics functionality in COMSOL, using the Peng– Robinson equation of state and the Brokaw model with high pressure correction for the viscosity. The temperature dependent viscosity for the brine is taken to be the viscosity of the Water material from COMSOL Multiphysics' material library. The pressure and temperature dependent density of the brine is approximated using a thermal expansion coefficient of 6·10-4 1/K, a compressibility of 4·10-10 1/Pa, and a reference density of 1040 kg/m3 at 1·105 Pa and 360 K. Dissolution of CO2 into the brine is not taken into account in this model. The relative permeabilities and capillary pressure are assumed to be given by the Brooks and Corey capillary pressure model, with the brine being the wetting phase.

2.2 Development of Malay Basin and injection well in COMSOL software.

There are three phases in the development of the model for part of Malay Basin in COMSOL software, which are creating the aquifer geometry and injection well, specifying the properties of sandstone aquifer, supercritical carbon dioxide and brine, and meshing of the whole geometry using physics-controlled condition. Figure 1 shows the final created geometry for the 10km2 sandstone aquifer of Malay Basin.

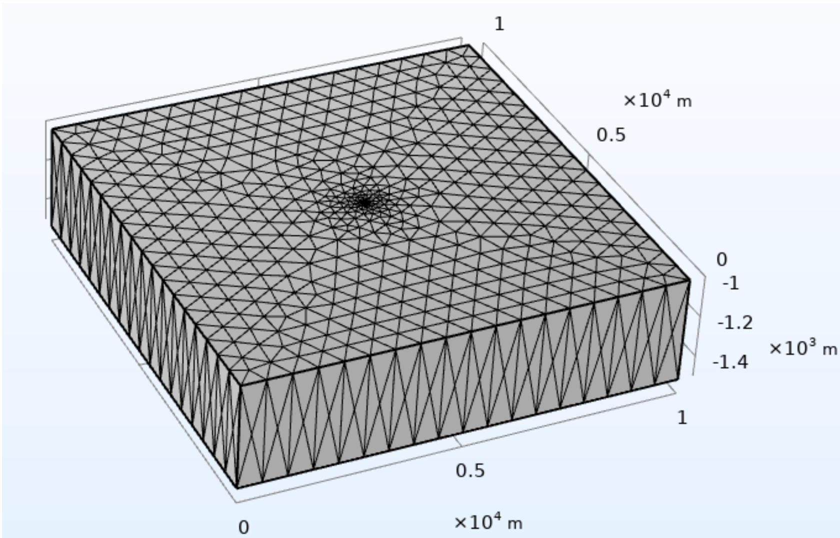

Figure 1. Geometry of Malay Basin created in COMSOL.

2.3 Setting up Multiphysics Component for the Model.

There are two physics that were grouped under the multiphase flow porous media physics in COMSOL software. The first one is Darcy's Law to incorporate the movement of CO2 through porous rock formations and provides a mathematical relationship between flow rate, pressure gradient, fluid viscosity, and porous media properties, such as permeability and porosity. The next physics is the phase transport in porous media that involves studying the movement and interaction of different fluids or gases within a porous material and understanding phenomena such as capillary pressure, which influences the distribution of fluids, and relative permeability that affects their flow rates.

2.4 Parametric Study.

Four different injection rates of CO2 were introduced into the sandstone aquifer with constant rate for 50 years and subsequently observed until 100 years. The injection rates used in this simulation are 25kg/s, 50kg/s, 75kg/s and 100kg/s. These sets of computation are carried out to identify the relationship between several key parameters which includes CO2 plume dispersion shape, radius, velocity and saturation with distance to the different injection rates. The time step of observation is set so that the CO2 plume properties can be identified at critical time; during injection (25 years), after injection was stopped (50 years), awhile after injection stopped (75 years) and long after injection stopped (100 years).

3 Result and Discussion

The crucial results which were computed from COMSOL software are Darcy's velocity magnitude and saturation of the CO2 plume migration in the sandstone aquifer of Malay Basin and is discussed herein as well as the verification of the obtained results.

3.1 Radius and Shape of CO2 Plume Dispersion.

From the results obtained for the radius of CO2 plume dispersion (Figure 2), the higher the injection rate, the wider the radius of CO2 dispersion.

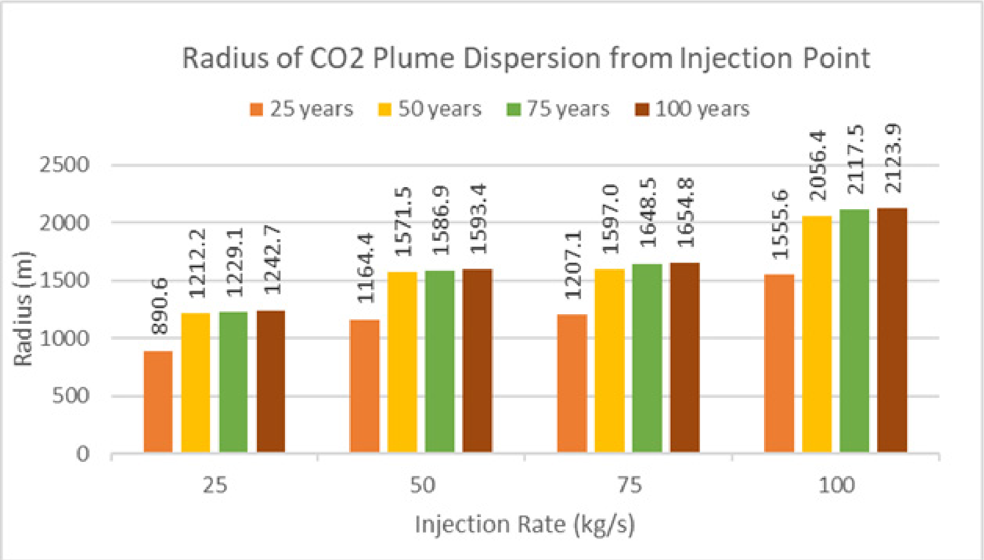

Figure 2. Radius of CO_2 Plume Dispersion with different injection rates at every 25 years up until 100 years.

In addition, the radius of CO2 plume migration also increases with time for respective injection rates. CO2 plume spread rapidly during the injection period, and nearly doubled the value of radius dispersed at 25 years to when the injection was stopped (50 years). This applies for all different injection rates. After the injection has stopped, CO2 plume still disperses but much slower and does not show very significant change of radius of CO2 dispersion. Additionally, for each of the different sets of models with varying injection rates, they all depict the same pattern and shape of CO2 plume migration. One set of examples for top view and front view of the CO2 dispersion in the sandstone aquifer is as displayed in Figure 3. According to the shape of CO2 plume dispersion observed from the 2D plot, the injected CO2 phase first migrates towards the reservoir's highest point due to buoyancy before being hydrodynamically confined below the restricting layer of cap rock. The cap rock, which is a no-flow border in this instance, traps the CO2 just below it [25]. The CO2 then diffuses laterally and partially dissolves in the reservoir fluids. The brine migrates downhill because of CO2 dissolving, increasing brine density, until it settles at the reservoir bottom [26].

Comparing the result obtained from this project and to the results obtained from the study by [21], the shape of CO2 plume migration for both studies are the same. The IPPC special report on carbon dioxide capture and storage (SRCCS) in 2005 identified buoyancy as the main driving force for CO2 plume migration in the two-phase region at distances far away from the well and in the long term. This driving force creates the iconic flared-funnel plume shape as CO2 rises buoyantly and spreads laterally until trapped under large-scale caprock formations. According to [27], the lateral spread of a CO2 plume is directly influenced by the pressure gradients in both the horizontal and vertical directions. The horizontal pressure gradient arises from radial flow, while the vertical pressure gradient is a result of the density difference between CO2 and brine. Assuming isotropic permeability laterally and vertically, the horizontal velocity of CO2 decreases as it moves away from the injection well due to the decreasing pressure gradient. On the other hand, the vertical velocity of CO2 remains constant, primarily driven by the density difference. As the distance from the well increases, there comes a point where the magnitudes of the horizontal and vertical CO2 velocities become comparable. At this stage, a significant amount of CO2 starts moving upward. Further from the well, the vertical pressure gradient becomes dominant over the horizontal pressure gradient, causing most of the CO2 to move vertically.

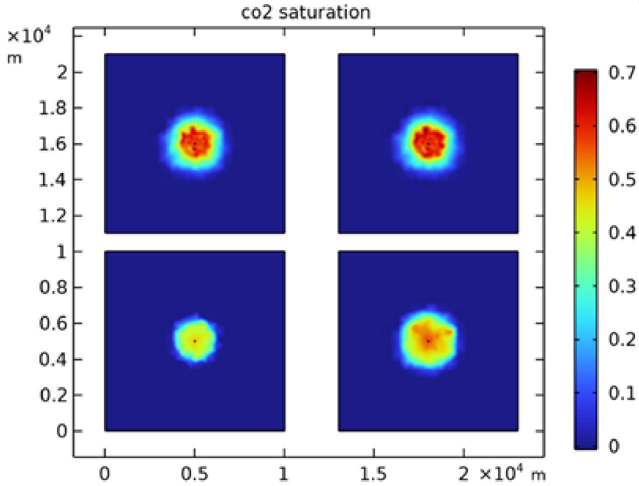

(a)

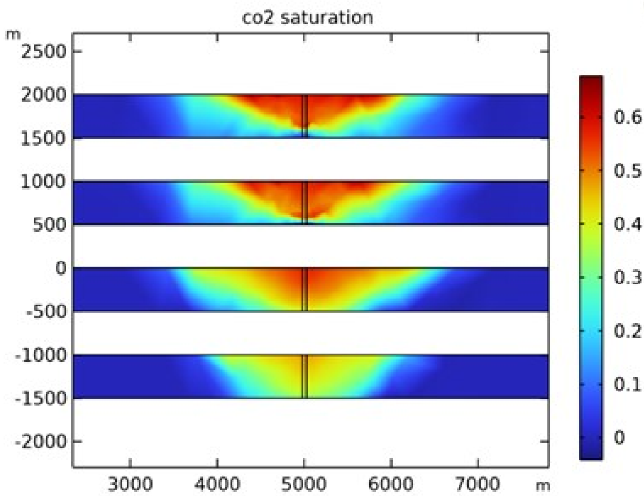

(b)

Figure 3. (a) Top view of the aquifer showing CO2 saturation with injection rate of 100 kg/s after 25 years (bottom left), after 50 years (bottom right), after 75 years (top left) and after 100 years (top

right). (b) Front view of the aquifer showing CO2 saturation with injection rate of 100 kg/s after 25, 50, 75 and 100 years (bottom to top).

3.2 Velocity of CO2 with different injection rates.

Figure 4 shows the result for velocity-distance plot of injected CO2 into the aquifer. Firstly, the result obtained for 25 years (during injection); higher injection rate achieved peak velocity at the position of injection well.

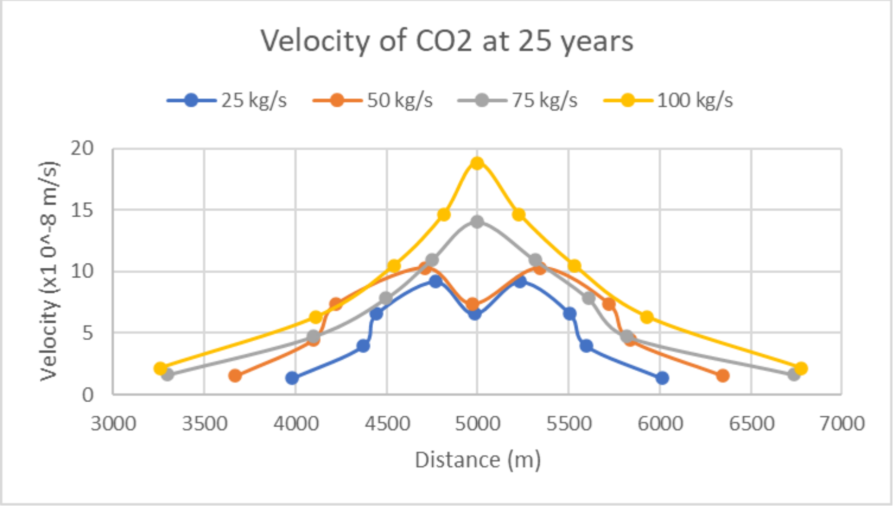

(a)

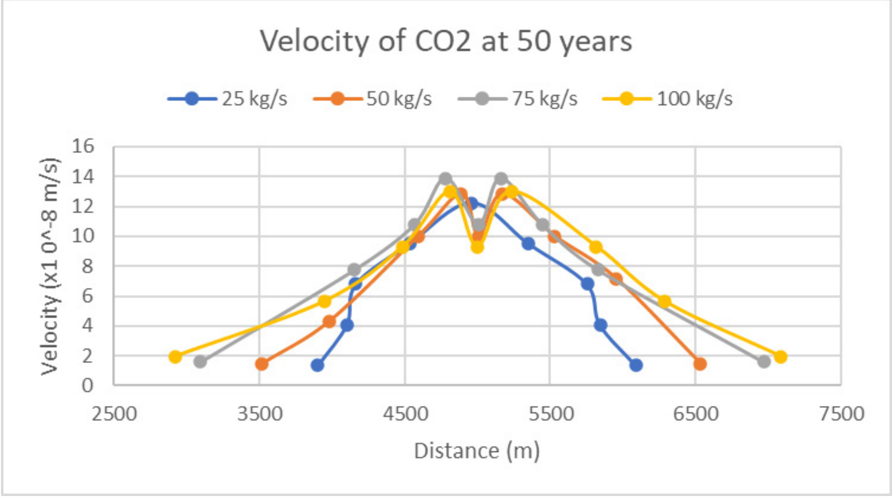

(b)

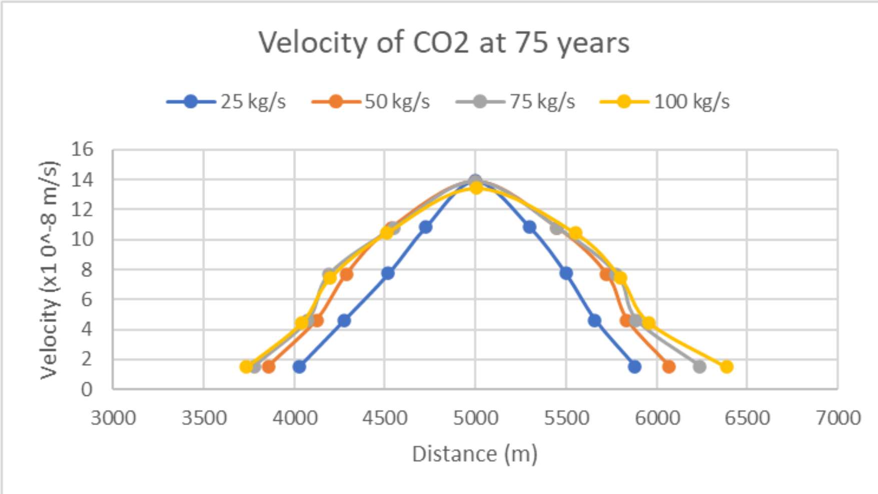

(c)

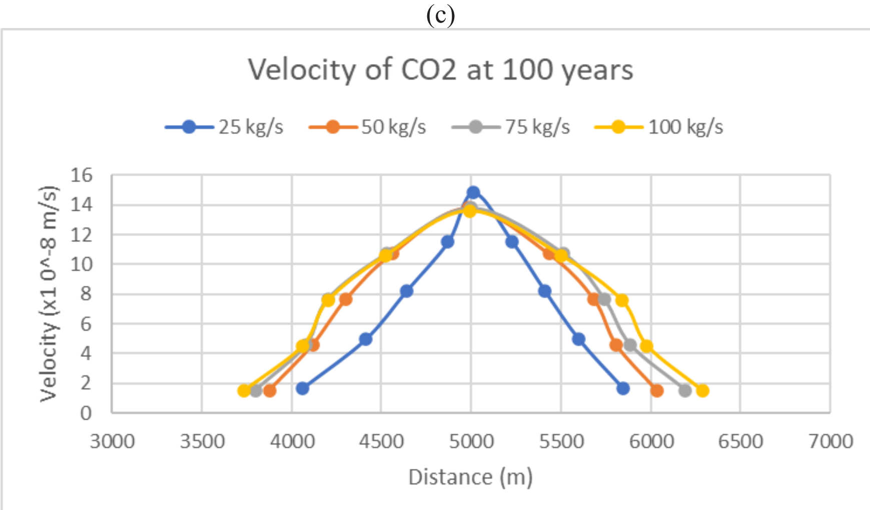

(d)

Figure 4. The velocity of CO2 with distance at (a) 25 years (b) 50 years (c) 75 years (d) 100 years from injection for different injection rates (25 kg/s, 50 kg/s, 75 kg/s and 100 kg/s).

One of the factors is due to the pressure gradient. When CO2 is injected into an aquifer, it creates a pressure gradient where the pressure is higher near the injection well and gradually decreases with distance from the well [28]. This pressure gradient drives the flow of CO2 through the aquifer, resulting in higher velocities near the injection point. Additionally, initially, the injected CO2 may not have had sufficient time to disperse or diffuse into the surrounding aquifer. As a result, the CO2 plume is more concentrated near the injection well, leading to higher velocities as it moves through a more confined area. However, there are also instances where the velocity values at the position of injection well are lower and only reach its peak velocity at certain distance away from the injection well. This can be observed for injection rate of 25 kg/s and 50 kg/s. It somehow formed an M-shaped plot in the velocity-distance graph. Specifically, the phenomenon arises due to resistance near the injection well caused by constriction effects and mixing with groundwater, leading to an initial reduction in velocity before increasing further from the injection well. These findings highlight the need for detailed consideration of near-well dynamics in CO2 injection designs. This phenomenon could be attributed by a few factors, one of it is the injection well itself can act as a constriction point or a source of flow resistance. Injection wells can exhibit flow resistance, resulting in a higher-pressure requirement to lift brine from the injection layer. This means that a greater pressure increase is necessary to overcome the resistance and enable the upward movement of brine from the injection zone [29]. This can cause a decrease in velocity near the injection well as the CO2 is forced through a smaller opening or encounters obstructions within the well. In addition, as the CO2 is injected into the aquifer, it may initially mix and disperse with the surrounding groundwater. This mixing process can lead to a dilution of the CO2 and a decrease in its velocity near the injection well. As the CO2 travels further away from the injection point, the mixing and dispersion effects may diminish, resulting in higher velocities.

After the injection has stopped (50 years), the velocity-distance plot for injection rate of 50kg/s, 75kg/s and 100kg/s all exhibits the "M" shape plot which indicates that the velocity at the injection well position is relatively lower, and the peak velocity is reached at a distance away from the injection well. This phenomenon referred to the same scenario as the aforementioned reason for injection rate of 25kg/s and 50kg/s at 25 years. It is mainly influenced by the constriction point at injection well and initial mixing and dilution of injected CO2 with the formation's groundwater which leads to a lower CO2 plume velocity at the position of injection well. However, only injection rate of 25kg/s shows that the CO2 plume reached its peak velocity at well position and decrease in velocity as it moves away. One possible explanation is that the injection rate of 25 kg/s allows for a slower and more controlled release of CO2 into the subsurface. This lower injection rate might result in a more concentrated and focused plume, leading to higher velocities as the CO2 propagates through the formation.

Next, for the velocity-distance plot of CO2 plume dispersion at 75 years and 100 years, all the injection rates depicted the same pattern of plot. The peak velocity is achieved at the position of injection well and slowly decreases as it migrates away laterally. Moreover, we can also observe that higher injection rates of supercritical CO2 into the aquifer tend to yield higher velocity of CO2 plume migration. This is because a higher injection rate introduces a larger volume of CO2 into the aquifer, resulting in increased flow and transport dynamics [30]. With a higher injection rate, there is a greater influx of CO2 into the aquifer, which creates a higher-pressure gradient. The increased pressure gradient drives the flow of CO2 through the aquifer at a faster rate, which then leads to higher velocities as the plume spreads away from the injection well. Other than that, the injected CO2 tends to follow the path of least resistance, which is often along the existing pore spaces, fractures, or other permeable pathways in the aquifer. These pathways are typically more abundant and interconnected near the injection well, providing less resistance to flow and facilitating higher velocities [31]. However, at 100 years, injection rate of 25kg/s showed the highest peak velocity which is 14.83 x 10-8 m/s compared to other higher injection rates. The same reasoning is applied like the case of velocity-distance plot at 50 years. A lower injection rate tends to generate a more localized and concentrated plume of CO2 as it moves through the formation. This concentrated plume can contribute to higher velocities compared to scenarios with higher injection rates. On the other hand, higher injection rates such as 50 kg/s, 75 kg/s, and 100 kg/s may lead to a more dispersed and diffused plume. This dispersion could potentially result in lower peak velocities as the CO2 is spread over a wider area.

To validate and compare our obtained data, we examined a study conducted by [32]. From the result obtained in their study, it can be inferred that CO2 injected with higher injection rate yielded a shorter breakthrough time. This means that with high injection rate, injected CO2 takes shorter time to travel through a given distance. Since the time taken to travel a given distance is inversely proportional to velocity, this also means that higher injection rate will result in higher velocity. The same scenario also mostly applies to the result obtained in this project since the highest injection rate (100kg/s) almost gives the highest velocity of CO2 migration all the time. All in all, it's important to consider that the behavior of CO2 in subsurface formations is complex and can be influenced by various factors, including the geological characteristics of the reservoir, fluid dynamics, and other site-specific conditions. A more comprehensive analysis is necessary to fully understand the reasons behind the observed velocities and the impact of injection rates on CO2 migration.

3.3 Saturation of CO2 with different injection rates.

From the plotted graph in Figure 5, all the different injection rates yield the same pattern of saturation decrement with distance. The saturation of CO2 being highest near the injection well is a result of the injection process and the fluid flow dynamics within the aquifer.

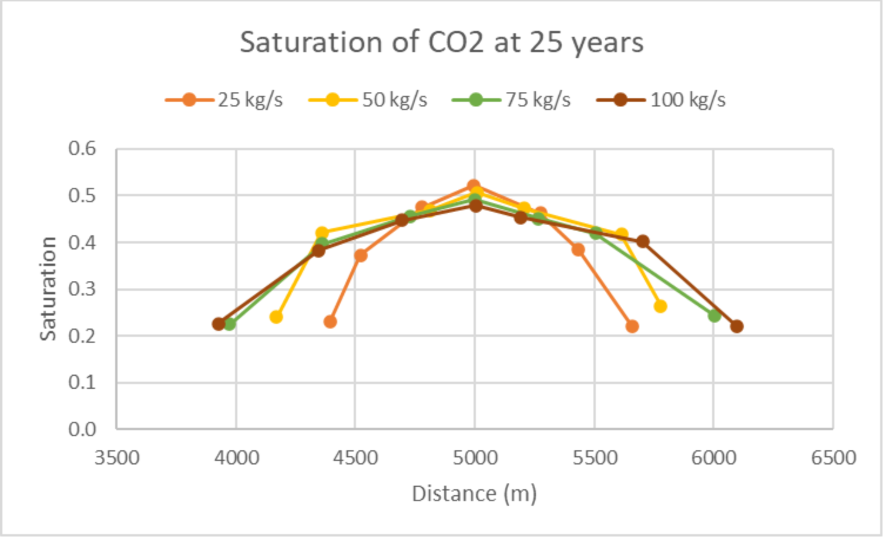

(a)

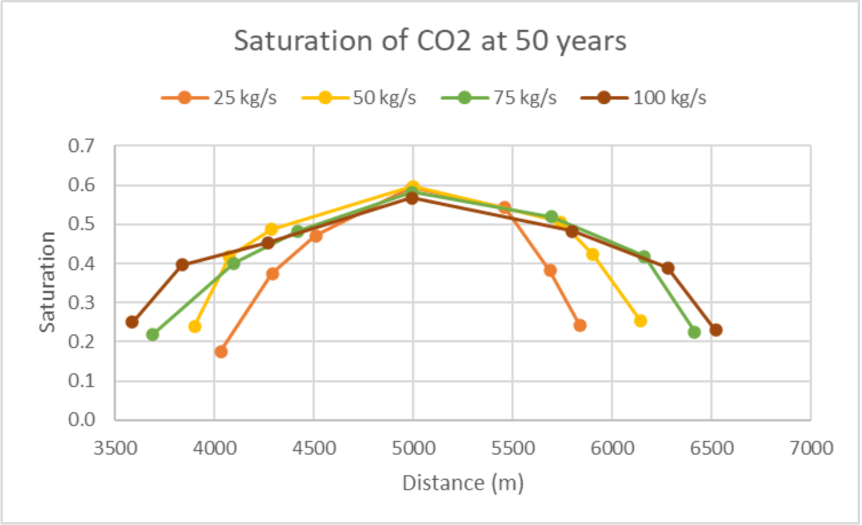
Saturation of CO2 at 50 years
25 kg/s
50 kg/s
75 kg/s
100 kg/s
Saturation
0.7
0.6
0.5
0.4
0.3
0.2
0.1
0.0
3500
4000
4500
5000
5500
6000
6500
7000
Distance (m)

(b)

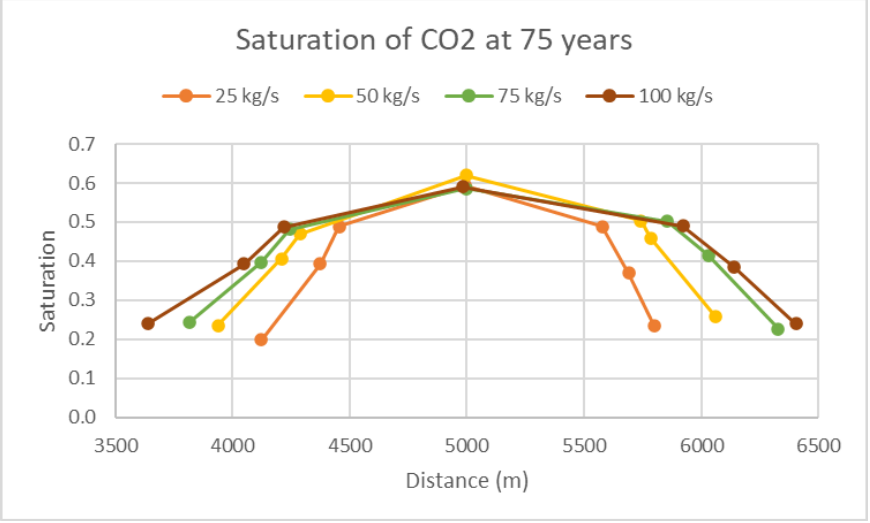
Saturation of CO2 at 75 years
25 kg/s
50 kg/s
75 kg/s
100 kg/s
Saturation
0.7
0.6
0.5
0.4
0.3
0.2
0.1
0.0
3500
4000
4500
5000
5500
6000
6500
Distance (m)

(c)

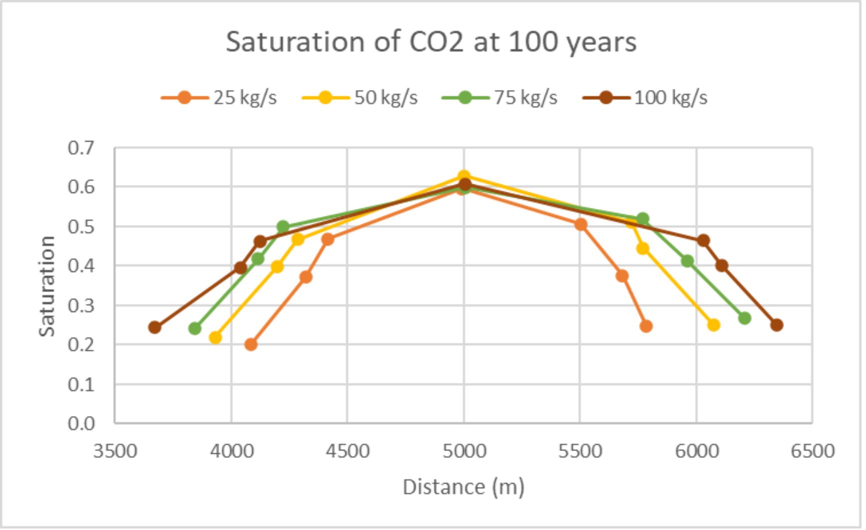

(d)

Figure 5. Plot of CO2 saturation with distance at (a) 25 years, (b) 50 years, (c) 75 years, and (d) 100 years with different injection rates (25 kg/s, 50 kg/s, 75 kg/s and 100 kg/s)

Several factors contribute to this phenomenon and one of them is when CO2 is injected into the aquifer, it enters the formation with a high concentration near the injection well. This high initial concentration creates a localized region of high saturation near the injection point. Near the injection well, these processes may not have had sufficient time to disperse the CO2 effectively, resulting in higher saturation levels in the immediate vicinity of the well [33]. After that, CO2 tends to spread out and disperse through the aquifer due to diffusion and dispersion processes. Furthermore, in the initial stages of injection, the fluid flow within the aquifer near the injection well might be relatively limited compared to later stages when the injected CO2 spreads further. Limited fluid flow can restrict the movement and spread of CO2 away from the well, causing higher saturation levels in the nearby region. Other than that, according to [28], there is typically a pressure gradient established around the injection well during injection, with higher pressure near the wellbore and decreasing pressure with distance. This pressure gradient can drive the CO2 to migrate preferentially toward regions of lower pressure, resulting in higher saturation near the injection well.

On the other hand, among all the injection rates, the highest injection rate (100kg/s) mostly leads to lowest peak saturation at the position of the well bore. This could be influenced by several factors. When a high injection rate is employed, there is a greater volume of injected CO2 entering the formation near the wellbore. This larger volume of CO2 can mix and disperse with the existing formation fluids [34], diluting the CO2 concentration and resulting in a lower saturation at the injection well location. Furthermore, higher injection rates can lead to faster flow velocities near the injection well. According to [35], the increased flow velocity can cause the injected CO2 to move more quickly away from the wellbore, reducing the time available for it to accumulate and saturate the surrounding formation.
Another obvious pattern of the saturation-distance plot of the CO2 plume dispersion is that the higher injection rate would occupy broader area and has higher saturation as it moves

away from the injection point. A study by [36] suggests that higher injection rates introduce a larger volume of CO2 into the subsurface formation over a given time period. This increased supply of CO2 allows for a greater potential for saturation to occur as the CO2 spreads and migrates through the formation. Furthermore, higher injection rates can propel the CO2 further away from the injection point within a given timeframe. As CO2 travels a greater distance, it has more opportunities to interact with the formation, filling a larger portion of the pore space and leading to a broader saturation zone. Table 1 shows the summary of the findings.

Table 1. Summary of the simulation findings.

Injection Rate (kg/s)	Maximum Plume Radius (m)	Maximum Velocity (m/s)
25	1,220	14.83 x 10-8
50	1,520	16.42 x 10-8
75	1,880	18.74 x 10-8
100	2,110	20.25 x 10-8

A similar result was also computed by COMSOL as a benchmark study for the Johansen Formation. Their results shows that saturation of CO2 is seen to spread broader with time like what has been computed from our study for Malay Basin. However, the pattern of the CO2 saturations differs, for the Johansen formation, the CO2 is seen to disperse unevenly after few years from injection while in our study, the CO2 migrates almost circularly from the injection point. This is because the part of Malay Basin modelled in our study is taken to have isotropic permeability and porosity both horizontally and vertically. While for Johansen Formation computed by COMSOL, they plotted the real porosity and permeability for the aquifer which typically varies for different formations. Hence, this resulted in the uneven distribution shape of CO2 plume saturations. Moreover, the maximum saturation for the Johansen formation is approximately 0.8 while for Malay Basin is only 0.63 as obtained from this study. This is because deeper injection depths typically result in higher reservoir pressures which enhance the solubility of CO2 in the formation fluids as mentioned by [37], potentially leading to higher CO2 saturation. The study’s results align with other modeling studies, such as those conducted on the Johansen Formation and the Bunter Sandstone Formation. Further validation using local field data from the Malay Basin is critical to enhance the reliability of the model predictions. However, we have limited field data from Malay Basin as it is confidential.

4 Conclusion

In this paper, an innovative model that employed the multiphysics component of multiphase flow in porous media multiphysics interface for tracking the fate of injected carbon dioxide plume in Malay Basin sandstone aquifer was proposed. This developed model serves as a potential and more practical alternative to laboratory or experimental works for assessing the migration of sequestered carbon dioxide. Findings conforming to the objectives of this study can be summarized as below:

1. CO2 plume migration within a deep saline aquifer is primarily upwards due to buoyancy and increased density of brine due to dissolution of CO2. This vertical migration continues before the CO2 is constrained by hydrodynamic trapping under the caprock. With the presence of pressure gradient due to injection, the CO2 proceeds with lateral dispersion. Over time and with higher injection rates, the radius of CO2 dispersion also increases.
2. The velocity of CO2 plume dispersion typically peaks at the injection point and decreases as it moves away laterally. However, factors such as constriction point at the well, insufficient breakthrough pressure can delay distance to achieve peak velocity. CO2 plume velocity then tends to decrease with distance due to pressure gradients and CO2 dissolution into the brine within the formations.
3. The saturation of CO2 is highest at the injection point because the injected CO2 initially does not have sufficient time to disperse as it is driven upwards due to buoyancy. Higher injection rate yields higher saturation of CO2 and occupies broader distance in a given time due to the higher volume injected.

This study concludes that, the numerical model for analysing the fate of injected CO2 in the sandstone aquifer of Malay Basin using COMSOL software is feasible and practical to be considered for further development. The findings have implications for both policymakers and engineers. Policymakers can leverage the results to draft guidelines for CO2 injection projects, emphasizing safety and efficacy. Engineers can use the insights to design injection protocols that optimize plume stability and minimize risks.

Acknowledgement

We would like to express my gratitude and appreciation to the Centre of Tropical Geoengineering for the support and encouragement. Special thanks to Universiti Teknologi Malaysia for funding this research under UTM Research Grant Tier 2, Vot number Q.J130000.2651.16J84.

References

1. Lindsey, R. (2022). Climate Change: Atmospheric Carbon Dioxide. Climate.gov; NOAA. https://www.climate.gov/news-features/understanding-climate/climate-change-atmospheric-carbon-dioxide
2. Alasinrin Babatunde, K., Faizah Said, F., Ghani, N., Nor, M., Rawshan, A., & Begum. (2019). Reducing Carbon Dioxide Emissions from Malaysian Power Sector: Current Issues and Future Directions (Mengurangkan Pengeluaran Karbon Dioksida dalam Sektor Tenaga di Malaysia: Isu Semasa dan Arah Masa Hadapan). Jurnal Kejuruteraan SI, 1(6), 59–69. https://www.ukm.my/jkukm/wp-content/uploads/2018/si1/6/8.pdf
3. Soong, Y., Howard, B. H., Hedges, S. W., Haljasmaa, I., Warzinski, R. P., Irdi, G., & McLendon, T. R. (2014). CO2 Sequestration in Saline Formation. Aerosol and Air Quality Research, 14(2), 522–532. https://doi.org/10.4209/aaqr.2013.06.0195
4. IPCC. (2005). Bert, M., Ogunlade, D., Heleen C., Manuela, L, & Leo, M. (Eds.), Carbon Dioxide Capture and Storage: Special Report of the Intergovernmental Panel on Climate Change (pp. 431-431). Cambridge University Press, UK.
5. National Academies of Sciences, Engineering, and Medicine. (2019). Negative Emissions Technologies and Reliable Sequestration: A Research Agenda. Washington, DC: The National Academies Press. https://doi.org/10.17226/25259.

6. Celia, M. A., Bachu, S., Nordbotten, J. M., & Bandilla, K. W. (2015). Status of CO2storage in deep saline aquifers with emphasis on modeling approaches and practical simulations. Water Resources Research, 51(9), 6846–6892. https://doi.org/10.1002/2015wr017609
7. Salvi, B. L., & Jindal, S. (2019). Recent developments and challenges ahead in carbon capture and sequestration technologies. SN Applied Sciences, 1(8). https://doi.org/10.1007/s42452-019-0909-2
8. Wilson, E. J., Johnson, T. L., & Keith, D. W. (2003). Regulating the Ultimate Sink: Managing the Risks of Geologic CO2Storage. Environmental Science & Technology, 37(16), 3476–3483. https://doi.org/10.1021/es021038+
9. Ajayi, T., Gomes, J. S., & Bera, A. (2019). A review of CO2 storage in geological formations emphasizing modeling, monitoring and capacity estimation approaches. Petroleum Science, 16(5), 1028–1063. https://doi.org/10.1007/s12182-019-0340-8
10. Szulczewski, M., & Juanes, R. (2009). A simple but rigorous model for calculating CO2 storage capacity in deep saline aquifers at the basin scale. Energy Procedia, 1(1), 3307–3314. https://doi.org/10.1016/j.egypro.2009.02.117
11. Soong, Y., Hedges, S. W., Howard, B. H., Dilmore, R. M., & Allen, D. E. (2013). Effect of contaminants from flue gas on CO2sequestration in saline formation. International Journal of Energy Research, 38(9), 1224–1232. https://doi.org/10.1002/er.3140
12. Michael, K., Golab, A., Shulakova, V., Ennis-King, J., Allinson, G., Sharma, S., & Aiken, T. (2010). Geological storage of CO2 in saline aquifers—A review of the experience from existing storage operations. International Journal of Greenhouse Gas Control, 4(4), 659–667. https://doi.org/10.1016/j.ijggc.2009.12.011
13. Torp TA, Gale J. (2004). Demonstrating storage of CO2 in geological reservoirs: the Sleipner and SACS projects. Energy. 2004;29(9):1361–9. https://doi.org/10.1016/s0360-5442(04)00153-7.
14. Bachu, S., Gunter, W. D., & Perkins, E. H. (1994). Aquifer disposal of CO2: Hydrodynamic and mineral trapping. Energy Conversion and Management, 35(4), 269–279. https://doi.org/10.1016/0196-8904(94)90060-4
15. Oldenburg, C. M. (2012). Geologic Carbon Sequestration geologic/geological carbon sequestration: Sustainability and Environmental Risk. Encyclopedia of Sustainability Science and Technology, 4119–4133. https://doi.org/10.1007/978-1-4419-0851-3_200
16. Hasbollah, D. Z. A. and Junin, R. (2015). A preliminary basin scale evaluation framework of potential sedimentary basins in Malaysia for carbon dioxide sequestration, Chemical Engineering Transactions 45, pp 1537-1542.
17. Kartikasurja, D. O., Lin, T. G., Sukahar, M. W., & Viratno, B. (2008). Study of Produced CO2 Storage into Aquifer in an Offshore Field, Malaysia. Onepetro.org; OnePetro. https://doi.org/10.2118/114553-MS
18. Das, D. B., Gill, B. S., Abidoye, L. K., & Khudaida, K. J. (2014). A numerical study of dynamic capillary pressure effect for supercritical carbon dioxide-water flow in porous domain. AIChE Journal, 60(12), 4266–4278. https://doi.org/10.1002/aic.14577
19. Birkholzer, J., Zhou, Q., & Tsang, C. (2009). Large-scale impact of CO2 storage in deep saline aquifers: A sensitivity study on pressure response in stratified systems. International Journal of Greenhouse Gas Control, 3(2), 181–194. https://doi.org/10.1016/j.ijggc.2008.08.002
20. Bachu, S., & Adams, J. J. (2003). Sequestration of CO2 in geological media in response to climate change: capacity of deep saline aquifers to sequester CO2 in solution. Energy Conversion and Management, 44(20), 3151–3175. https://doi.org/10.1016/s0196-8904(03)00101-8
21. Naderi Beni, A., Kühn, M., Meyer, R., & Clauser, C. (2011). Numerical Modeling of a Potential Geological CO 2 Sequestration Site at Minden (Germany). Environmental Modeling & Assessment, 17(4), 337–351. https://doi.org/10.1007/s10666-011-9295-x
22. Ranjith, P. G., Perera, M. S. A., & Khan, E. (2012). A study of safe CO2storage capacity in saline aquifers: a numerical study. International Journal of Energy Research, 37(3), 189–199. https://doi.org/10.1002/er.2954
23. Pruess, K., Garcia, J., Kovscek, T., Oldenburg, C., Rutqvist, J., Steefel, C., & Xu, T. (2002). Intercomparison of numerical simulation codes for geologic disposal of CO2. Www.osti.gov. https://www.osti.gov/biblio/813566
24. Junin, R. and Hasbollah, D. Z. A. (2016). CO2 Storage Capacity Assessment of Deep Saline Aquifers in Malaysia [Paper presentation]. World Academy of Science, Engineering and Technology, WASET 2016, London.

25. Wang, Y., Vuik, C., & Hajibeygi, H. (2022). Analysis of hydrodynamic trapping interactions during full-cycle injection and migration of CO2 in deep saline aquifers. Advances in Water Resources, 159, 104073. https://doi.org/10.1016/j.advwatres.2021.104073
26. Yongqiang, T., Zihao, L., Wang, R., Cui, M., Wang, X., Lun, Z., & Lu, Y. (2019). Experimental Study on the Density-Driven Carbon Dioxide Convective Diffusion in Formation Water at Reservoir Conditions. ACS Omega, 4(6), 11082–11092. https://doi.org/10.1021/acsomega.9b00627
27. Frailey, S. M., & Leetaru, H. (2009). Geological factors affecting CO2 plume distribution. Energy Procedia, 1(1), 3107–3112. https://doi.org/10.1016/j.egypro.2009.02.091
28. Azaroual, M., André, L., Peysson, Y., Pironon, J., Broseta, D., Dedecker, F., Egermann, P., Desroches, J., & Hy-Billiot, J. (2012). Behaviour of the CO2 injection well and the near wellbore during carbon dioxide injection in saline aquifers. Hal-Brgm.archives-Ouvertes.fr. https://hal-brgm.archives-ouvertes.fr/hal-00755073
29. Bandilla, K. W., Kraemer, S. R., & Birkholzer, J. T. (2012). Using semi-analytical solutions to approximate the area of potential impact for carbon dioxide injection. International Journal of Greenhouse Gas Control, 7. https://www.osti.gov/biblio/1210902
30. Samuel, R. J., & Mahgerefteh, H. (2019). Investigating the impact of flow rate ramp-up on carbon dioxide start-up injection. International Journal of Greenhouse Gas Control, 88, 482–490. https://doi.org/10.1016/j.ijggc.2019.04.025.
31. Zhang, Z. F., White, S. K., & White, M. D. (2015). Delineating the horizontal plume extent and CO2 distribution at geologic sequestration sites. International Journal of Greenhouse Gas Control, 43, 141–148. https://doi.org/10.1016/j.ijggc.2015.10.018
32. Teng, Y., Liu, Y., Lu, G., Suekane, T., Wang, D., & Song, Y. (2017). Experimental Evaluation of Injection Pressure and Flow Rate Effects on Geological CO2 Sequestration Using MRI. Energy Procedia, 114, 4986–4993. https://doi.org/10.1016/j.egypro.2017.03.1642
33. Azin, R., Mahmoudy, M., Raad, S. M. J., & Osfouri, S. (2013). Measurement and modeling of CO2 diffusion coefficient in Saline Aquifer at reservoir conditions. Open Engineering, 3(4). https://doi.org/10.2478/s13531-012-0069-2
34. Iglauer, S. (2011). Dissolution Trapping of Carbon Dioxide in Reservoir Formation Brine – A Carbon Storage Mechanism, Mass Transfer - Advanced Aspects, Dr. Hironori Nakajima (Ed.), ISBN: 978-953-307-636-2, InTech, Available from: http://www.intechopen.com/books/mass-transfer-advanced-aspects/dissolutiontrapping-of-carbon-dioxide-in-reservoir-formation-brine-a-carbon-storage-mechanism
35. Zhu, T., Ajo-Franklin, J., Daley, T. M., & Marone, C. (2019). Dynamics of geologic CO 2 storage and plume motion revealed by seismic coda waves. Proceedings of the National Academy of Sciences, 116(7), 2464–2469. https://doi.org/10.1073/pnas.1810903116
36. Stanislaw Lasocki, & Orlecka-Sikora, B. (2020). High Injection Rates Counteract Formation of Far-Reaching Fluid Migration Pathways at The Geysers Geothermal Field. https://doi.org/10.1029/2019gl086212
37. Mohammadian, E., Hadavimoghaddam, F., Kheirollahi, M., Jafari, M., Chenlu, X., & Liu, B. (2023). Probing Solubility and pH of CO2 in aqueous solutions: Implications for CO2 injection into oceans. Journal of CO2 Utilization, 71, 102463. https://doi.org/10.1016/j.jcou.2023.102463